

---

# Diagnostic Imaging of the Esophageal Cancer

# 3

Hiroya Ojiri

---

## Abstract

Diagnostic imaging can play an important role in detecting and staging esophageal cancer. Current diagnostic workup consists of barium esophagography, endoscopy/endoscopic ultrasonography (EUS), computed tomography (CT), magnetic resonance imaging (MRI), and positron emission tomography (PET). CT, EUS, MRI, and PET should be considered complementary modalities. In combination, they are crucial to determine the most appropriate treatment for patients with esophageal cancer.

This chapter describes the diagnostic imaging, mainly of CT and MRI, and relevant anatomy of the esophagus for clinical decision making with regard to esophageal cancers. EUS precisely shows tumor invasion mainly localized in the esophageal wall (defined as T1-3). On the other hand, cross-sectional imaging such as CT and MRI is useful to detect tumor invasion to the adjacent structures beyond the adventitia (defined as T4). Currently, regional lymph node metastases are evaluated using EUS, CT, and/or FDG-PET. Detection of metastatic lymphadenopathies on CT depends primarily on nodal size (size criteria) although size is known to be an insensitive parameter. MRI's role to assess regional nodal metastasis is limited so far. CT is currently the best diagnostic method to detect metastases.

---

## Keywords

CT • Esophageal cancer • Imaging • MRI

---

H. Ojiri, MD (✉)

Department of Radiology, The Jikei University School of Medicine,  
3-25-8 Nishi-shimbashi, Minato-ku, Tokyo 105-8461, Japan  
e-mail: [ojiri@jikei.ac.jp](mailto:ojiri@jikei.ac.jp)

---

## 3.1 Introduction

Patients with esophageal cancer have a poor prognosis because it is usually detected at an advanced stage. Accurate preoperative staging is crucial in determining the most appropriate therapeutic strategy for each patient. Surgical resection is currently the best curative treatment for esophageal cancers without locoregionally advanced invasion or distant metastases. Inappropriate attempts of surgery must be avoided.

The radiologist can play an important role in detecting and staging esophageal cancer. Current diagnostic workup consists of barium esophagography, endoscopy/endoscopic ultrasonography (EUS), computed tomography (CT), magnetic resonance imaging (MRI), and positron emission tomography (PET). In combination, they are crucial to determine the most appropriate treatment for patients with esophageal cancer. CT, EUS, MRI, and PET should be considered complementary modalities. The main purpose of imaging studies in patients with esophageal cancer is to stage the disease as accurately as possible and to determine which patients may be suitable candidates for surgery. The accurate assessment requires knowledge of the advantages and limitations of each modality, an anatomy of the esophagus and spread patterns of esophageal cancer.

Squamous cell carcinoma (SCC) that is the most prevalent esophageal cancer worldwide mostly arises from the upper portion of the esophagus whereas adenocarcinoma primarily involves the lower portion and esophagogastric junction (EGJ). Hence, importance of a direct invasion to the tracheobronchial tree and metastatic adenopathy in the superior mediastinum should be emphasized in the imaging diagnosis of esophageal SCC.

This chapter describes the diagnostic imaging, mainly of CT and MRI, and relevant anatomy of the esophagus for clinical decision making with regard to esophageal cancers.

---

## 3.2 Anatomy of the Esophagus

### 3.2.1 Divisions of the Esophagus

The esophagus is a tubular structure between the esophageal verge and esophagogastric junction (EGJ), clinically divided into four segments [1]: cervical esophagus, upper thoracic esophagus, middle thoracic esophagus, and lower thoracic esophagus/EGJ. The cervical esophagus begins at the level of the inferior border of the cricoid cartilage and ends at the thoracic inlet. The upper thoracic esophagus begins at the thoracic inlet and ends at the level of the lower border of the azygos vein. The middle thoracic esophagus is bordered superiorly by the lower border of the azygos vein and inferiorly by the inferior pulmonary vein. The lower thoracic esophagus is bordered superiorly by the inferior pulmonary vein and inferiorly by the stomach. The lower end of the lower esophagus includes the EGJ.

The cricoid cartilage is an easy-to-recognize structure to identify the transition between the hypopharynx and the cervical esophagus (Fig. 3.1). The esophageal

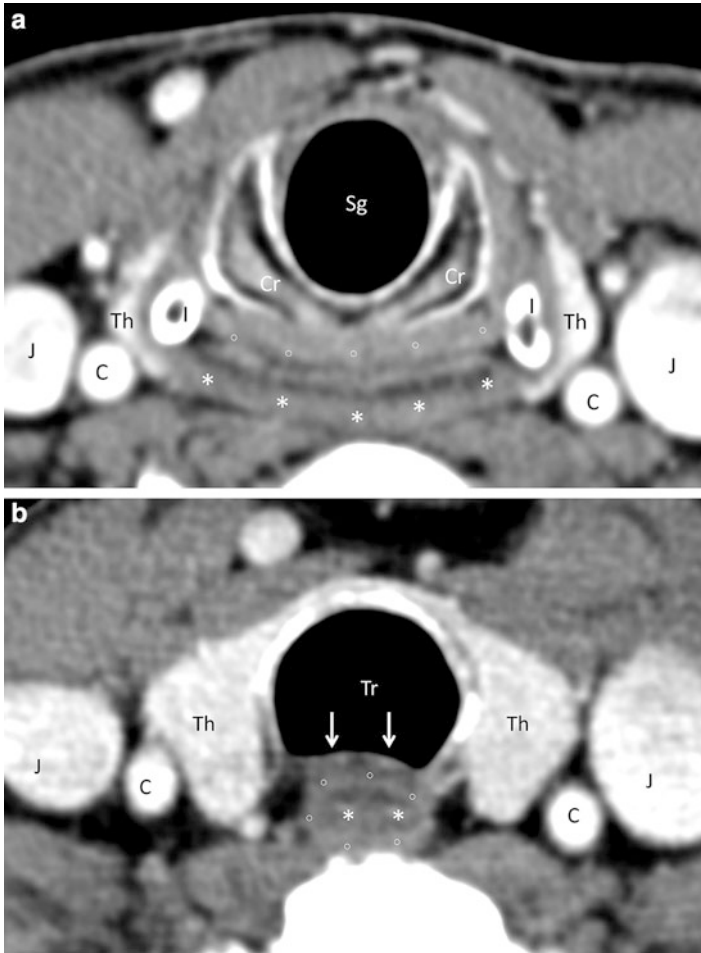


**Fig. 3.1** Normal CT anatomy of the hypopharynx and cervical esophagus. **(a)** Contrast-enhanced axial CT image obtained at the level of the hypopharynx. The ossified cricoid cartilage (Cr) is identified as a “U-shaped” structure at this level because the anterior arch is lower than the posterior lamina of cricoid cartilage. A posterior aspect of the subglottic laryngeal airway (Sg) is convex along the internal surface of the lamina of cricoid cartilage. The hypopharynx is a flattened ellipsoid structure on axial image as the inferior pharyngeal constrictor partly arises from the inferior cornu (I) of thyroid cartilage on both sides. The hypopharynx at this level consists of anterior “postcricoid portion (*open circle*)” and “posterior pharyngeal wall (*asterisk*).” C common carotid artery, J internal jugular vein, Th (superior pole of) thyroid gland. **(b)** Contrast-enhanced axial CT image of the cervical esophagus. The cervical esophagus identified as an oval structure posterior to the trachea (Tr) shows a circumferential zonal anatomy. It seemingly consists of three layers: an inner enhancing layer representing the mucosa (*asterisk*), outer soft tissue attenuation layer (*open circle*) representing the muscularis propria, and low-attenuation submucosal fat between them. A posterior aspect of the trachea is concave because of indentation of the cervical esophagus upon the membranous portion (*arrows*) of the trachea. C common carotid artery, J internal jugular vein, Th thyroid gland



**Fig. 3.2** Normal CT anatomy of the thoracic inlet. Contrast-enhanced axial CT image. The esophagus (E) deviates to the *left*, whereas the trachea (Tr) stays in the *middle*. C common carotid artery, Cl clavicle (sternal end), Sa subclavian artery, Sv subclavian vein

verge is at the lower margin of the cricopharyngeus muscle at the level of C6. The cricopharyngeus muscle is actually a specialized functional zone of inferior constrictor muscle that identifies this physiologic boundary. Cross-sectional images clearly depict such transition [2]; the hypopharynx is a flattened soft tissue ellipsoid structure attached to the posterolateral margin of the thyroid lamina and inferior cornu (Fig. 3.1a). On the other hand, the cervical esophagus creates an oval structure posterior to the trachea as the muscular wall loses its attachment to the thyroid cartilages (Fig. 3.1b). The trachea normally stays in the midline from the lower neck to the thoracic inlet, while the esophagus will often deviate to the left at this level (Fig. 3.2) [2].

### 3.2.2 Zonal Anatomy of the Esophageal Wall

The esophageal wall consists of mucosa, muscularis mucosae, submucosa, muscularis propria, and adventitia. EUS can differentiate such layers to determine the depth of tumor invasion into the esophageal wall (Fig. 3.3) [3]. Mucosal enhancement may be visible on contrast-enhanced CT (Figs. 3.1b and 3.2) and contrast-enhanced MRI.

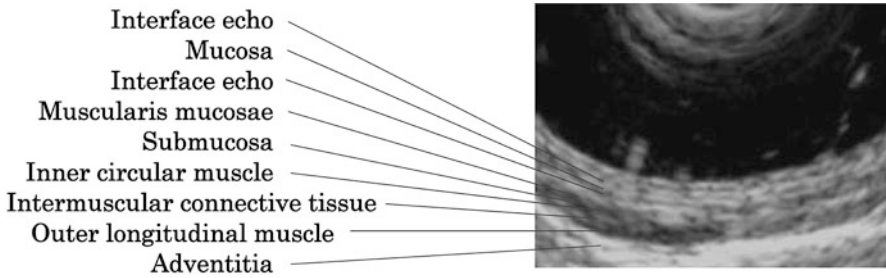


**Fig. 3.3** EUS of the normal esophagus (by courtesy of Dr. Gohda, Department of Endoscopy, The Jikei University School of Medicine). EUS differentiates nine layers of the esophageal wall

### 3.3 T Staging by Imaging

T staging of the esophageal cancer is principally defined by depth of invasion. Because the esophagus lacks a serosa, there is no anatomic barrier to prevent rapid local invasion of the tumor into the mediastinum. As a result, esophageal cancer can easily spread to adjacent structures in the neck or thorax, including the trachea, thyroid gland, larynx, bronchi, aorta, lung, pericardium, and diaphragm [4]. Involvement of the adjacent structures in the mediastinum is classified as T4 disease which is further divided into two: resectable disease (T4a) and unresectable disease (T4b) [1].

An important goal of clinical T staging is the identification of tumor invasion of mediastinal structures, since affected patients may not be suitable candidates for surgical resection [5]. Depth of tumor invasion is one of the criteria used to select multimodality therapy instead of primary surgery [5].

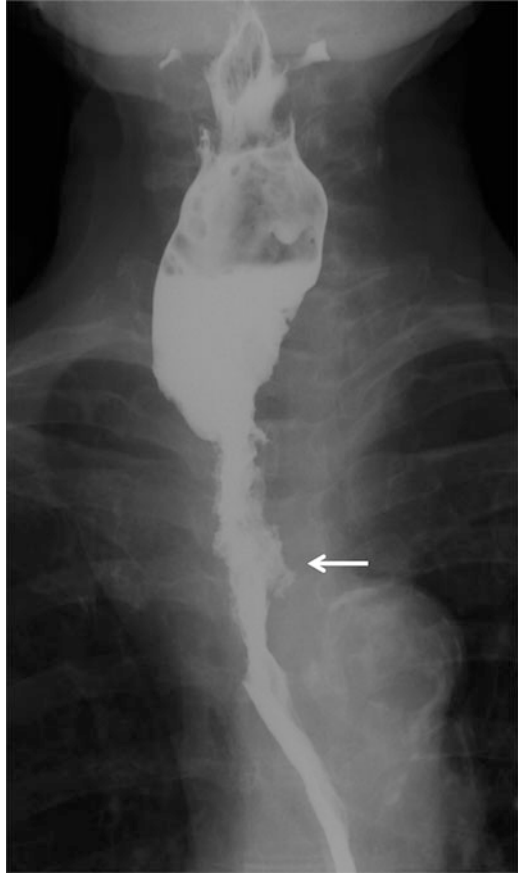
Imaging modalities should be complementary to stage the primary lesion; EUS precisely shows tumor invasion mainly localized in the esophageal wall (defined as T1-3). On the other hand, cross-sectional imaging such as CT and MRI is useful to detect tumor invasion to the adjacent structures beyond the adventitia (defined as T4). This chapter mainly focuses on CT and MRI.

#### 3.3.1 Barium Esophagography

Barium esophagography is commonly performed as an initial examination to evaluate patients with dysphagia/odynophagia which may be the first manifestation of esophageal cancer.

Single-contrast technique is suitable to assess passage and wall rigidity and characterize strictures. Double-contrast technique allows the assessment of mucosal irregularity such as elevated and ulcerative lesions although double-contrast images of good quality may not be obtained distal to high-grade obstructive disease.

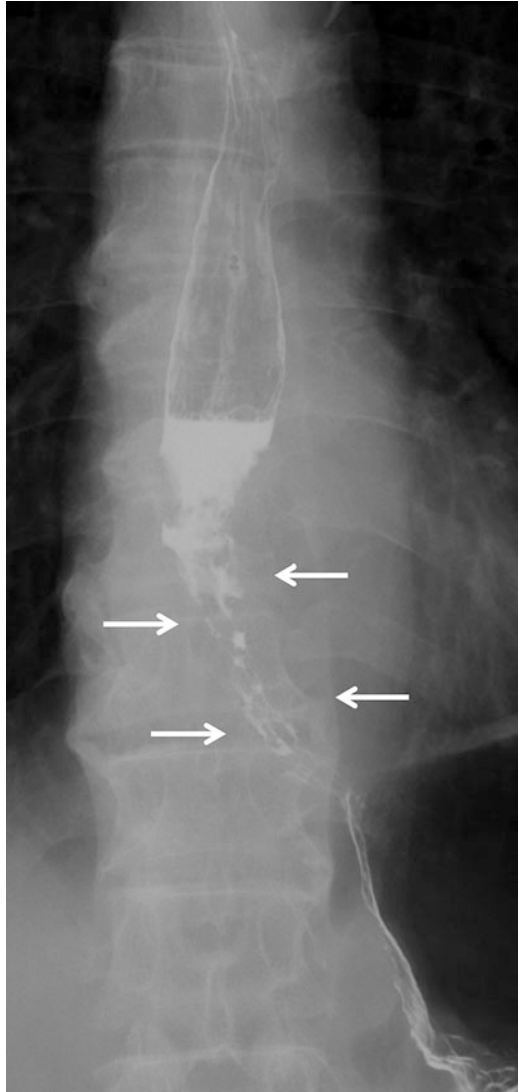
**Fig. 3.4** Esophageal cancer (upper thoracic esophagus). On single-contrast barium esophagography there is an irregular stricture of the esophagus (Ut) associated with ulceration (*arrow*)



Barium esophagography is very helpful to determine longitudinal extent and location of the disease relative to anatomical landmarks such as the tracheal bifurcation; to which esophageal division does the lesion belong? This is necessary to set an appropriate field of radiotherapy (RT).

On esophagograms, early esophageal cancers manifest as small polypoid or plaquelike lesions or superficial spreading lesions, whereas advanced esophageal cancers manifest as infiltrating, polypoid, ulcerative, or varicoid lesions (Figs. 3.4 and 3.5) [6]. Typical findings of advanced diseases include an irregular stricture (Figs. 3.4, 3.5, and 3.6a), mass-like filling defect (Fig. 3.7a), or ulcer (Fig. 3.4) on single-contrast images, and an abrupt change in caliber and contour (Fig. 3.6b) or irregularly shaped mass on double-contrast images. The Japan Esophageal Society uses a classification system based on the macroscopic appearance of esophageal cancer [7].

**Fig. 3.5** Esophageal cancer (lower thoracic esophagus). Barium esophagography shows an irregular stenosis and varicoid appearance of the lower thoracic esophagus (arrows)



Double-contrast esophagography has a sensitivity of greater than 95 % in the detection of esophageal cancer [8]. When malignancy suggested on barium esophagogram, a positive predictive value is approximately 40 %. And endoscopically proven esophageal cancers were found on barium esophagogram in 98 % [8, 9].

The synchronous second primary lesion must be carefully inspected. Tracheoesophageal fistula may be demonstrated when resulting from the tumor invasion (Fig. 3.8a).



**Fig. 3.6** Esophageal cancer (middle thoracic esophagus). Single-contrast image (a) and double-contrast image (b) of barium esophagography reveal an irregular stricture and abrupt caliber change of the middle thoracic esophagus (*arrows*)

### 3.3.2 EUS

EUS allowing visualization of the distinct layers of the esophageal wall (Fig. 3.3) can accurately demonstrate the depth of tumor invasion. It is useful in distinguishing T1 and T2 lesions.

However, EUS has several limitations in T staging: one is that the accuracy is highly operator dependent and another is evaluation of non-traversable, stenotic tumors. There is a known failure rate of 14–25 % because of stenotic lesions that prevent the passage of the endoscope [10, 11], EUS and CT should be used as complementary methods for TNM staging of esophageal cancer [12].

EUS is also useful to determine regional lymph node involvement. Combined use of fine-needle aspiration and EUS can improve assessment of lymph node involvement [5].

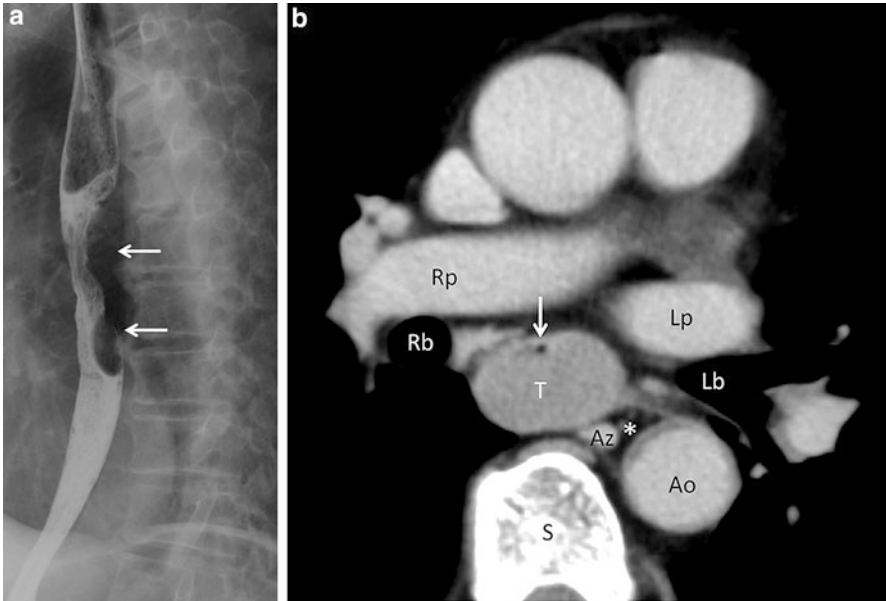


**Fig. 3.7** Esophageal cancer (middle thoracic esophagus). (a) Barium esophagography shows an irregularly shaped, mass-like filling defect (*arrows*) in the lower thoracic esophagus. (b) Contrast-enhanced axial CT image at the level of the middle thoracic esophagus. Asymmetrical wall thickening forms a soft tissue mass (*T*) in the distended middle thoracic esophagus. Narrowing esophageal lumen is identified as an eccentric area of air density (*arrow*). A fat plane around the esophagus is entirely preserved, and a triangular fat space (*asterisk*) among the esophagus, aorta (*Ao*), and spine (*S*) is also maintained. Such findings exclude T4 disease with high degree of confidence. *Az* azygos vein, *Lb* left main bronchus, *Lp* left pulmonary artery, *Rb* right main bronchus, *Rp* right pulmonary artery

### 3.3.3 CT

Patients with esophageal cancer are best staged by CT, despite recognizing difficulties in determining local irresectability and mediastinal node involvement [13–15]. With the advent of multi-detector CT, it allows more accurate staging of the disease [5]. CT has been the mainstay for staging newly diagnosed esophageal cancer. The increasing use of EUS and PET has improved the staging algorithm for it. Currently, combined use of CT, EUS, and PET is advocated to determine whether a patient should be treated with surgery, chemotherapy, or a chemoradiation therapy [5].

In practice, CT is recommended for initial imaging following confirmation of esophageal cancer at pathologic analysis. The N and M status can be evaluated by CT at the same time.

CT is limited in determining the exact depth of tumor infiltration of the esophageal wall and considered to be unable to adequately help differentiate between T1, T2, and T3 disease. However, CT is useful to distinguish between T3 and T4 lesions and to rule out unresectable (T4a) or distant metastatic disease (Figs. 3.7b and 3.9a).

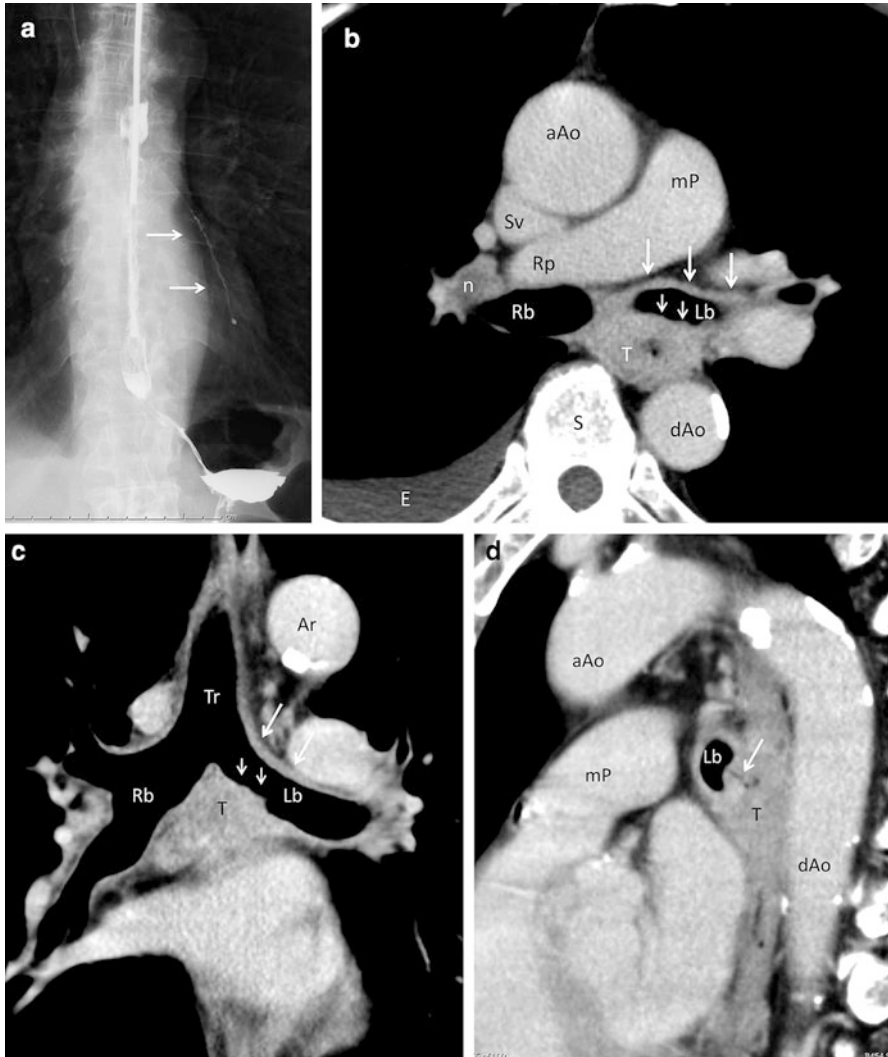


**Fig. 3.8** Esophageal cancer (middle thoracic esophagus). Esophagography (a) shows contrast material leaking into the left main bronchus and lower lobe bronchi (arrows). Contrast-enhanced axial CT image at the level just below the tracheal bifurcation (b) and coronal image at the level of the tracheal bifurcation (c) show an irregular and circumferential wall thickening of the esophagus representing esophageal cancer (T). An irregular interface (small arrows) between the tumor (T) and air density within the left main bronchus (Lb) and diffusely infiltrative change (large arrows) along the left main bronchus strongly suggest bronchial invasion. Metastatic hilar adenopathy (n) and right pleural effusion (E) are also noted (b). Reformatted sagittal image (d) well depicts a fistula (arrow) between the tumor (T) and a posterior aspect of left main bronchus (Lb). aAo ascending aorta, Ar aortic arch, dAo descending aorta, mP main pulmonary artery, Rb right main bronchus, Rp right pulmonary artery, S spine, Sv superior vena cava

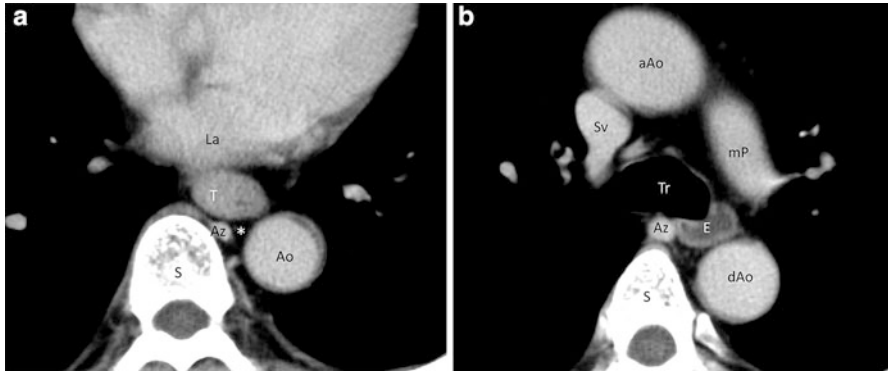


**Fig. 3.9** Esophageal cancer (lower thoracic esophagus). **(a)** Contrast-enhanced axial CT image at the level of Lt shows asymmetrical wall thickening of the lower thoracic esophagus (*T*). Integrity both of an entire fat plane around the esophagus and of a triangular fat space (*asterisk*) among the esophagus, aorta (*Ao*), and spine (*S*) is maintained, excluding T4 disease. *Az* azygos vein, *La* left atrium. **(b)** Contrast-enhanced axial CT image at the level of the tracheal bifurcation. The esophagus (*E*) proximal to the esophageal cancer (**a**) is distended with fluid attenuation. The esophagus at this level has even thin wall measuring approximately 2 mm. *aAo* ascending aorta, *Az* azygos vein, *dAo* descending aorta, *mP* main pulmonary artery, *S* spine, *Tr* trachea

### 3.3.3.1 CT Study Protocol and Optimal Phase for the Evaluation

CT examination should be inclusive from the neck through the entire upper abdomen to evaluate T, N, and M factors. Intravenous administration of contrast material is necessary. Optimal timing of image acquisition is a little bit controversial, depending on what should be evaluated by CT. Pre-contrast and post-contrast of delayed phase images are sufficient to evaluate N and M factors. On the other hand, some investigators recommend an arterial phase (on dynamic study) to detect the primary lesion (T factor) which may be better evaluated by EUS.

Umeoka et al. reported that the 2nd arterial phase of dynamic CT (35 sec after attenuation of 200HU was obtained at the descending aorta) is the optimal phase for visualization of esophageal cancer [16]. In their other report early esophageal rim enhancement on arterial phase of dynamic CT that was identified only in T3/T4 diseases could improve preoperative differentiation between T1/T2 and T3/T4 diseases [17].

Holsher et al. reported that the sensitivity values of the T staging in the arterial phase were 0 % in T1a, 71.4 % in T1b, 12.5 % in T2, 89.5 % in T3, and 100 % in T4. The sensitivity values in the venous phase were 0 % in T1a, 14.3 % in T1b, 0 % in T2, 94.7 % in T3, and 100 % in T4 [12].

Venous phase images are necessary to evaluate mediastinal adenopathies and metastatic liver tumors. Yoon et al. reported that 80 % of esophageal cancers were detectable on post-contrast CT in the venous phase although nearly 70 % of T1 lesions were missed [18].

### 3.3.3.2 Diagnostic Criteria of the Esophageal Cancer

#### Esophageal Wall Thickness

In general, CT is considered incapable of distinguishing the layers of the esophageal wall. Wall thickening of the esophagus is the most important CT feature to detect the esophageal cancer and its (mainly, longitudinal) extent. Precise localization of the esophageal cancers is helpful for planning radiation therapy.

Generally, any esophageal wall thicker than 5 mm is considered abnormal (Figs. 3.7b, 3.8b, and 3.9a) [19]. Wall thickness more than 5 mm is the criterion for abnormal wall thickening of the esophagus, suggested by an M.D. Anderson study without consideration of the status of the esophagus [20, 21]. Moss et al. proposed criteria as follows: the esophageal wall thicker than 5 mm is abnormal on CT images (Moss stages II); thickness of the esophageal wall between 3 and 5 mm indicated early lesions that did not make the wall apparently thickened (Moss stages I) [22].

The esophageal wall thickness seems to largely depend on the status of the esophagus. The esophageal wall thicker than 3 mm is abnormal when the esophagus is distended [22, 23]. Xia et al. reported that normal esophagus has a wall thickness around 5 mm in contraction status, 3 mm in dilatation (Fig. 3.9b) and roughly no more than 5.5 mm in any status [20]. In their study the largest wall thickness of the esophagus was 4.70 mm in contraction and 2.11 mm in dilatation. When dilating, the esophageal wall thickness was between 1.87 and 2.70 mm and the cervical esophageal wall was the thickest. When contracting, wall of the abdominal esophagus is thicker than the cervical and thoracic esophagus. They also reported that average of esophageal wall thickness was about 1 mm larger in males than females. Age and the thickness of subcutaneous fat had no significant impact on the esophageal wall thickness [20].

Asymmetric wall thickening of the esophagus is a primary but nonspecific CT finding of esophageal cancer (Figs. 3.7a and 3.9a) [5].

#### Other Features

High-resolution, post-contrast CT of good quality may differentiate three layers of the esophageal wall; a well-enhancing inner layer, fat-attenuation middle layer, and poorly enhancing outer layer representing the mucosa, submucosal fat, and muscularis propria, respectively (Figs. 3.1b, 3.2, and 3.10). An external contour of the outer layer should be surrounded by the adventitia. Theoretically, understanding of such zonal anatomy helps estimating depth of tumor invasion for T staging of the esophageal cancer. When the outer layer (muscularis propria) is preserved, the disease is assigned as T1 (Fig. 3.11). When the outer layer is partly encroached by a moderately enhancing tumor, the disease is assigned as T2. The transmural tumor invasion of the outer layer (muscularis propria) suggests T3 disease (Figs. 3.12 and 3.13) when the external contour of the esophagus is smooth and/or fat planes around the esophagus are preserved and T4 disease when the external contour of the esophagus is irregular and fat planes between the esophagus

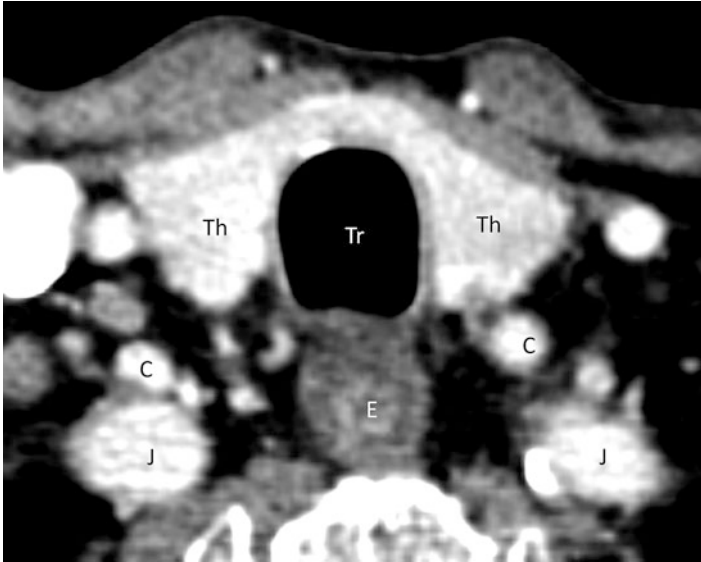


**Fig. 3.10** Zonal anatomy of the esophageal wall on CT. Contrast-enhanced axial CT image of the cervical esophagus reveals three different layers of the esophageal (*E*) wall: the inner enhancing layer, middle fatty layer, and outer soft tissue density layer representing the mucosa, submucosal fat, and muscularis propria, respectively. *C* common carotid artery, *J* internal jugular vein, *Th* thyroid gland, *Tr* trachea

and adjacent structures are obliterated (Figs. 3.8 and 3.14). However, such differentiation of each layer of the esophageal wall is not always possible.

A dilated fluid- and debris-filled esophageal lumen may be noted proximal to an obstructing disease (Fig. 3.9).

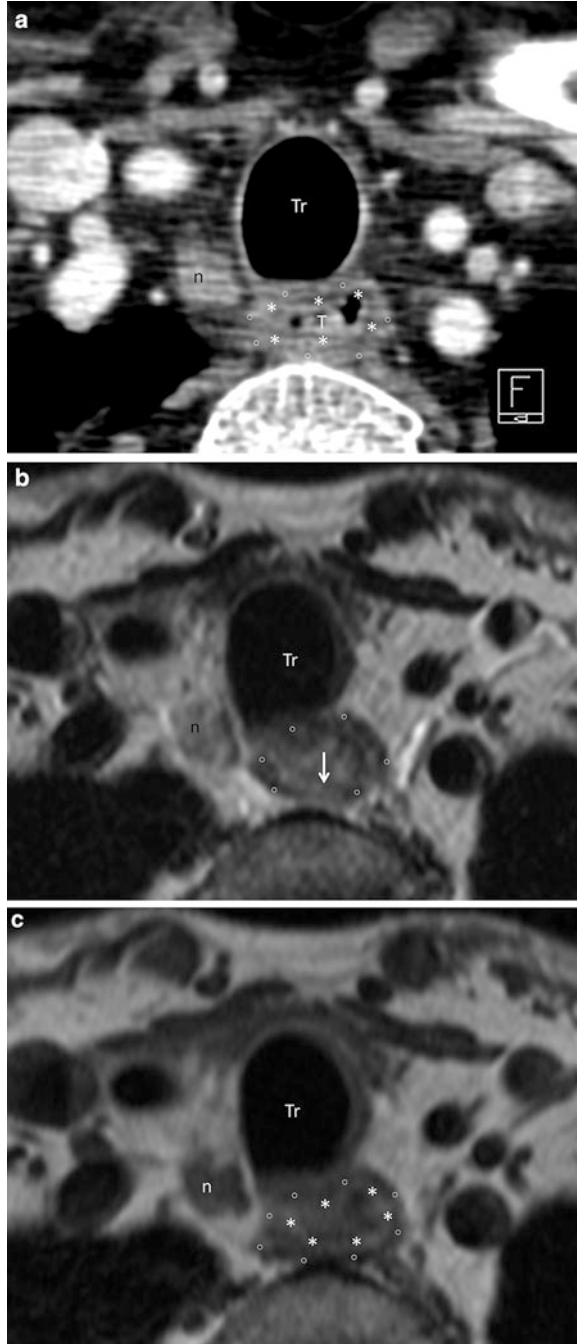
### 3.3.3.3 Diagnostic Criteria for Tumor Invasion to the Adjacent Structures

It is essential to evaluate resectability of the primary lesion when considering appropriate treatment strategy for patients with esophageal cancer. Tumor invasion to the mediastinal structures such as the aorta (Fig. 3.15) and tracheobronchial tree (Figs. 3.8, 3.14a, 3.16, and 3.17) is crucial.

CT is fairly reliable in determining resectability by excluding T4b cancers (Figs. 3.7b and 3.9a) [23]. The CT criteria for local invasion include loss of fat planes between the tumor and adjacent structures in the mediastinum and displacement or indentation of other mediastinal structures. The sensitivity and specificity of CT for predicting mediastinal invasion of the esophageal cancer are 88–100 % and 85–100 %, respectively [24, 25]. The sensitivity, specificity, and accuracy of CT for aortic invasion are 6, 85, and 58 %, respectively, and for tracheobronchial invasion are 31–100 %, 68–98 %, and 74–97 %, respectively [24, 27–29].

Although the presence of the fat plane rules out invasion (Figs. 3.7b and 3.9a), absence of the fat plane does not always indicate invasion. Nevertheless, tumor

**Fig. 3.11** Esophageal cancer (cervical esophagus; T1). Contrast-enhanced axial CT image of the level of the cervical esophagus (**a**) shows a nodular lesion (*T*) arising from the posterior aspect of esophageal wall. A fatty submucosal layer (*asterisk*) and soft tissue muscular layer (*open circle*) are entirely maintained. Metastatic adenopathy of the right paratracheal node (*n*) is noted. On T2-weighted axial image (**b**) the indistinct low-intensity muscular layer (*open circle*) at the posterior aspect (*arrow*) raises possibility of partial invasion of the muscularis propria (T2 disease). However, both the high-intensity submucosal fat (*asterisk*) and tissue-intensity muscular layer (*open circle*) are well preserved on T1-weighted image (**c**). Findings on T1-weighted axial image (**c**) exclude deep invasion to the muscularis propria and radiologically suggest T1 disease. *n* enlarged paratracheal node, *Tr* trachea



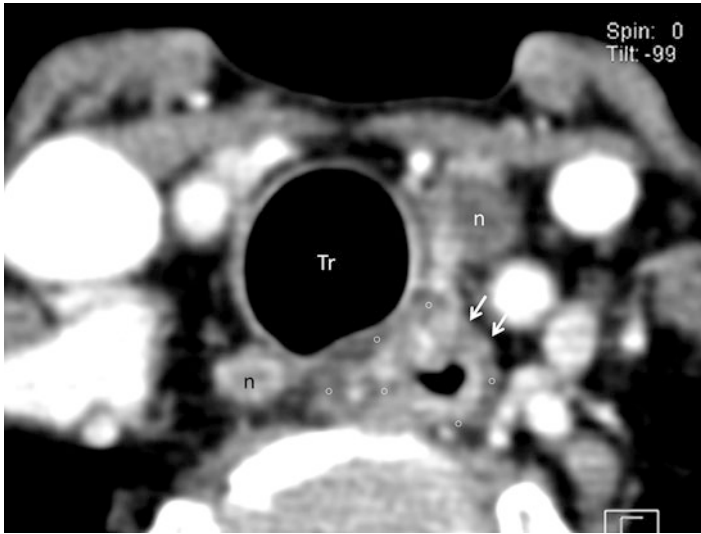


**Fig. 3.12** Esophageal cancer (cervical esophagus; T3). Contrast-enhanced axial CT image at the level of the cervical esophagus differentiates the inner enhancing mucosal layer and outer poorly enhancing muscular layer (*open circle*). The relatively thickened inner layer at the anterior aspect represents the primary lesion. A combination of a focal encroachment of the muscular layer (*arrows*) and smooth external contour of the esophagus suggests T3 disease. There are metastatic paratracheal nodes (*n*) on both sides. *Tr* Trachea

invasion is likely if the fat plane is obliterated at the site of probable invasion (Fig. 3.15b) and CT scans obtained immediately above and below that level show an intact fat plane [23]. We must notice that fat planes can be obliterated after radiotherapy/chemoradiotherapy or surgical intervention.

Lefor et al. reported that lesions more than 3.0 cm wide on CT scans were associated with a statistically significantly higher frequency of extraesophageal spread. The duration of survival was affected by lesion width and the presence of extraesophageal spread of disease [30]. Ruf et al. reported that esophageal cancer was unresectable when 4 contiguous CT sections demonstrated periesophageal infiltration [13, 31].

#### **Invasion to the Aorta (Defined as T4b)**

Aortic invasion by esophageal cancer detected at autopsy or during surgery varies from 2 to 20 % [13, 14, 25]. On CT, aortic invasion is suggested if 90° or more of the aorta is in contact with the tumor [25] or if there is obliteration of the triangular fat space between the esophagus, aorta, and spine adjacent to the primary lesion (Fig. 3.15) [28].

Picus et al. proposed the first criteria. They determined aortic invasion with approximately 80 % overall accuracy. Aortic invasion was diagnosed if the area of contact between the esophagus and the aorta created an arc of greater than 90°

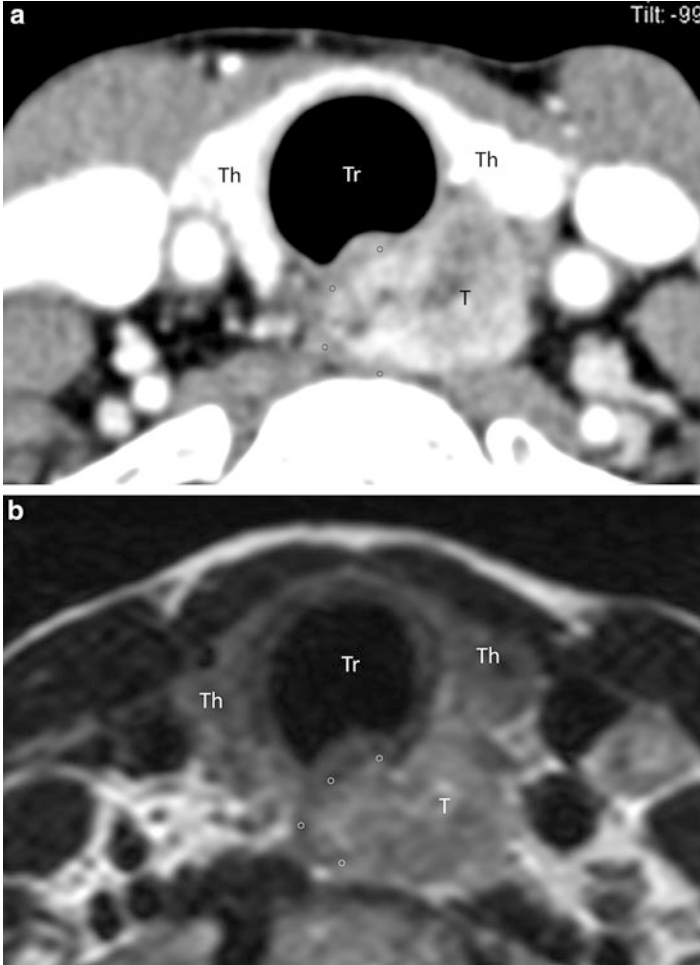


**Fig. 3.13** Esophageal cancer (cervical esophagus; T3). Contrast-enhanced axial CT image (a) and T2-weighted axial image (b) at the level of the cervical esophagus show an infiltrative tumor (T). No detectable muscular layer (*open circle*) on the *left side* without loss of tissue planes among the esophagus and adjacent structures is suggestive of T3 disease. *Th* thyroid gland, *Tr* trachea

(Fig. 3.15a). If the arc was less than  $45^\circ$ , aortic invasion was considered absent; an arc of  $45\text{--}90^\circ$  was considered indeterminate [25].

Takashima et al. proposed the second criteria: obliteration of the triangular fat space between the esophagus, aorta, and spine suggestive of aortic invasion (Fig. 3.15a). And they reported that both sensitivity (100 %) and specificity (86 %) for the MRI were high with such criteria; CT and MRI have the same accuracy in predicting resectability. In their study, no patients had a false-negative result (Figs. 3.7b and 3.9a) [28]. Ogawa et al. reported that the second criteria

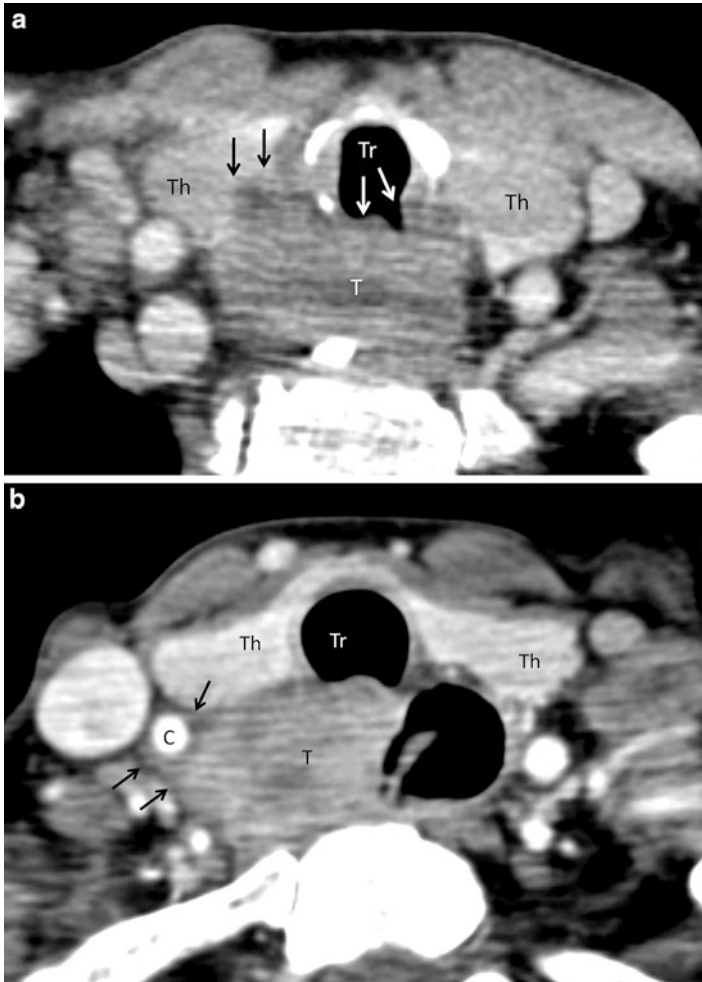


**Fig. 3.14** Esophageal cancer (cervical esophagus; T4). Contrast-enhanced axial CT image at the level of the cervical esophagus (**a**) shows an irregularly shaped mass (*T*). The mass anteriorly invades to the trachea (*Tr*) (*white arrows*) and right lobe of the thyroid gland (*Th*) (*black arrows*). Contrast-enhanced axial CT image at the level of the cervical esophagus of different patients (**b**). There is an eccentric mass (*T*) representing the primary lesion and possible metastatic adenopathy of the paraesophageal node. The tumor laterally encompasses more than two-thirds of the right common carotid artery (*C*) (*arrows*). Findings strongly suggest carotid invasion. *Th* thyroid gland, *Tr* trachea

(obliteration of the triangular fat space) were correlated with definitive invasion of the adventitia but not necessarily into the aorta itself and suggested that only when tumor is observed between the aorta and spine it strongly indicates the presence of aortic invasion [32].

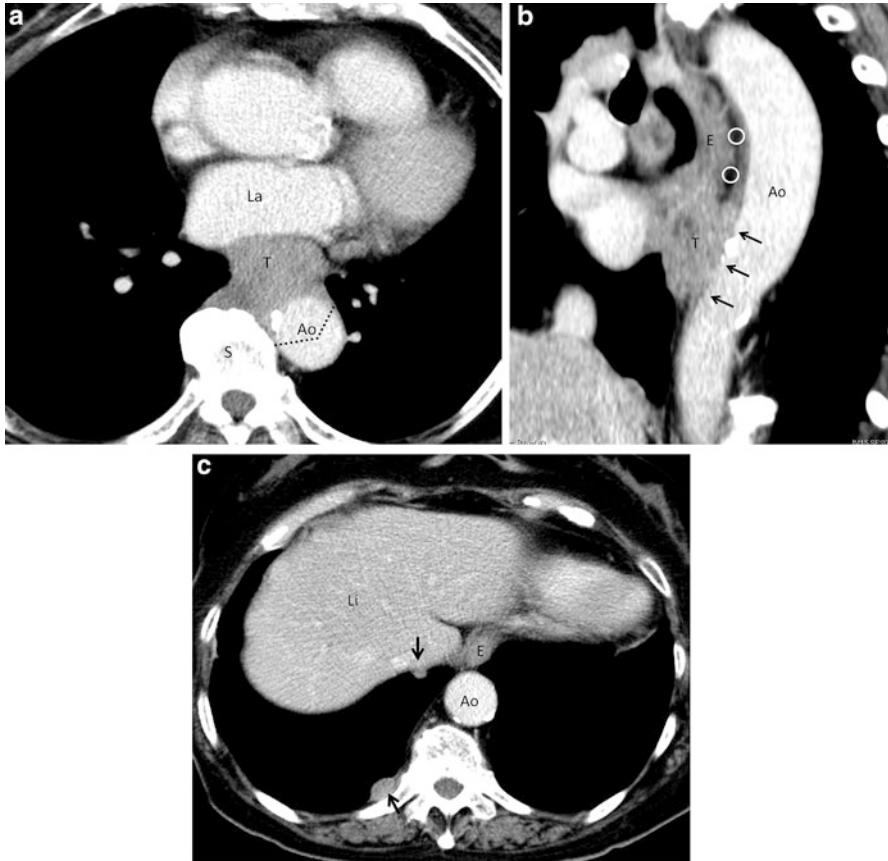


**Fig. 3.15** Esophageal cancer (middle and lower thoracic esophagus; T4). (a) Contrast-enhanced axial CT image at the level of the left atrium (*La*). There is an infiltrative tumor (*T*) of the esophagus in the posterior mediastinum. The tumor directly abuts upon the anterior aspect of the descending aorta (*Ao*) with obliteration of the triangular fat space (please see Figs. 3.7b and 3.9a) among the esophagus, aorta (*Ao*), and spine (*S*). The area of contact between the tumor (*T*) and aorta (*Ao*) creates an arc of approximately  $120^\circ$  (greater than  $90^\circ$ ); dotted lines creating “Picus angle”. Findings strongly suggest aortic invasion. Oblique sagittal image (b) shows that the tumor (*T*) broadly abuts upon the descending aorta (*Ao*) with obliteration (arrows) of fat plane (open circle) between the esophagus (*E*) and the aorta. Axial image at the level just above the diaphragm (c). There are several nodular tumor deposits (arrows) on the pleural surface on the right side, representing pleuritis carcinomatosa (pleural seeding). *Ao* descending aorta, *E* esophagus, *Li* liver

### Invasion to the Tracheobronchial Tree (Defined as T4b)

A tracheobronchial fistula (Figs. 3.8 and 3.17b) or tumor growth into the airway lumen (Fig. 3.14a) is a definite sign of tracheobronchial invasion. Displacement or indentation of the posterior wall of the trachea (Figs. 3.14a and 3.16) or bronchus (usually the left mainstem bronchus) (Figs. 3.8 and 3.17) by the tumor have also proved accurate in predicting tracheobronchial invasion (Fig. 3.8) [25].

**Fig. 3.16** Esophageal cancer (upper thoracic esophagus; T4). Contrast-enhanced axial CT image at the level of superior mediastinum shows irregular thickening of the esophageal wall (*T*). The tumor (*T*) indents the membranous portion (*asterisk*) and infiltrates along the right lateral wall (*arrows*) of the trachea (*Tr*). Such findings strongly suggest tracheal invasion

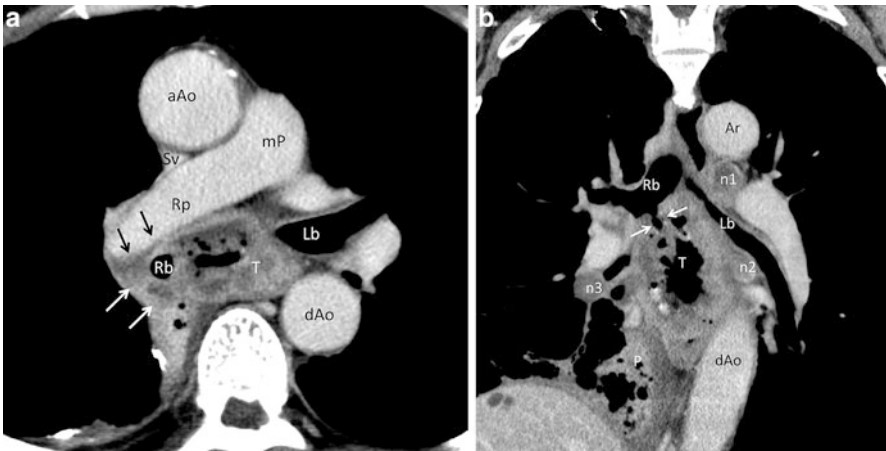


**Fig. 3.17** Esophageal cancer (middle thoracic esophagus; T4). (a) Contrast-enhanced axial CT image at the level of middle thoracic esophagus. A necrotic tumor (*T*) arising from the middle thoracic esophagus encompasses the right main bronchus (*Rb*) (*arrows*). *aAo* ascending aorta, *dAo* descending aorta, *Lb* left main bronchus, *mP* main pulmonary artery, *Rp* right pulmonary artery, *Sv* superior vena cava. (b) Reformatted coronal CT image. A tracheoesophageal fistula (*arrows*) between the tumor (*T*) and right main bronchus (*Rb*) is well depicted. Significant enlargement and internal low attenuation of the left tracheobronchial (*n1*), middle thoracic paraesophageal (*n2*), and right hilar nodes (*n3*), representing multiple metastatic adenopathies in the mediastinum and right pulmonary hilum. *Ar* aortic arch, *dAo* descending aorta, *P* (aspiration-induced) pneumonia in the right lung base

### **Invasion to the Other Structures**

Gastric invasion is manifested by a soft tissue mass extending from the primary esophageal tumor into the gastric fundus [28].

And pericardial invasion (defined as T4a) is diagnosed when pericardial thickening, pericardial effusion, or indentation of the heart with loss of pericardial fat plane is noted [5].

### **3.3.4 MRI**

MRI is superior to CT in evaluation of the cervical esophageal cancer because of its higher contrast resolution (Fig. 3.11). However, it is not much helpful in the thoracic esophagus and EGJ because it is often degraded by motion artifact. Currently, MRI has not yielded significant advantages compared to CT. The sensitivity and specificity of MRI for the determination of tumor invasion are roughly equivalent to those of CT. MRI and CT have nearly the same accuracy in predicting resectability of esophageal cancer [28]. Generally, MRI is considered not superior to CT for staging esophageal cancer [12]. MRI's role in the evaluation of esophageal cancer has been somewhat limited to date [24].

However, MRI's ability to depict esophageal cancer is continuously improving. MRI potentially complements the limitation of other imaging strategies [24]. Sakurada et al. reported that 1.5 T MRI examinations with faster sequences and cardiac/respiratory gating using both T2-weighted and diffusion-weighted images revealed T1 lesions in 33 %, T2 lesions in 58 %, T3 lesions in 96 %, and T4 lesions in 100 % [33].

T2-weighted axial images at the neck can differentiate two distinct layers of the cervical esophageal wall: a high-intensity inner layer and low-intensity outer layer representing a complex of the mucosa and submucosa and muscularis propria, respectively (Fig. 3.11). T3 disease is manifested by encroachment of the low-intensity outer layer (muscularis propria) with preservation of tissue planes between the tumor and adjacent structures (Fig. 3.13b), and T4 disease is manifested by encroachment of the outer layer with obliteration of tissue planes.

The areas of infiltrating tumor will usually enhance more than muscle. The submucosal extent of tumor is best appreciated on T2-weighted or contrast-enhanced T1-weighted MR images [2]. T1-weighted images may differentiate the submucosal fat as a high-intensity layer and muscularis mucosa as a tissue-intensity layer (Fig. 3.11) and complement T2-weighted images. Fat planes around the esophagus are best evaluated on T1-weighted images (Fig. 3.11c).

### **3.3.5 PET**

PET is useful for assessment of distant metastases but is inappropriate for detecting and staging primary tumors [5]. In general, it is impossible to detect tumor foci smaller than 5 mm on PET. The cost remains the primary limitation of PET.

### 3.4 N Staging by Imaging

The esophagus has an extensive lymphatic drainage system [5]. N factor is the most significant prognosticator in esophageal cancer.

Precise evaluation of the N status is difficult. Currently, regional lymph node metastases are evaluated using EUS, CT, and/or FDG-PET [24]. The most common sites of metastatic adenopathy in the mediastinum and around the celiac trunk (Fig. 3.18) often can be evaluated by CT and EUS [24]. EUS has been considered to be superior to CT in detection of metastatic lymph nodes [5]. However, using EUS, only lymph nodes close to the esophageal wall can be visualized whereas CT can demonstrate both regional and distant lymph node metastases (Fig. 3.18) [11]. And CT is superior to EUS for evaluating celiac nodes due to non-traversable stenoses [33]. Representative nodal groups on CT images are illustrated in Fig. 3.19.

Detection of metastatic lymphadenopathies on CT depends primarily on nodal size (size criteria) (Figs. 3.8b, 3.11, 3.12, and 3.17b) [5]. Lymph nodes larger than 1 cm in short-axis dimension are considered suggestive of metastatic disease although size is known to be an insensitive parameter for determining nodal spread because tumor can be present in subcentimeter nodes [35]. Generally, mediastinal and abdominal nodes are abnormal when a maximum axial diameter is greater than 1 cm [28]. A short-axis diameter greater than 1 cm is considered abnormal for mediastinal nodes except the subcarinal node in which 1.4 cm is the upper limit of normal. The sensitivity is 30–60 % and specificity is 60–80 % in most studies adopting 1 cm as size criterion to define an enlarged node on CT [36, 37]. We must recognize that enlargement of lymph nodes is nonspecific and can easily be reactive

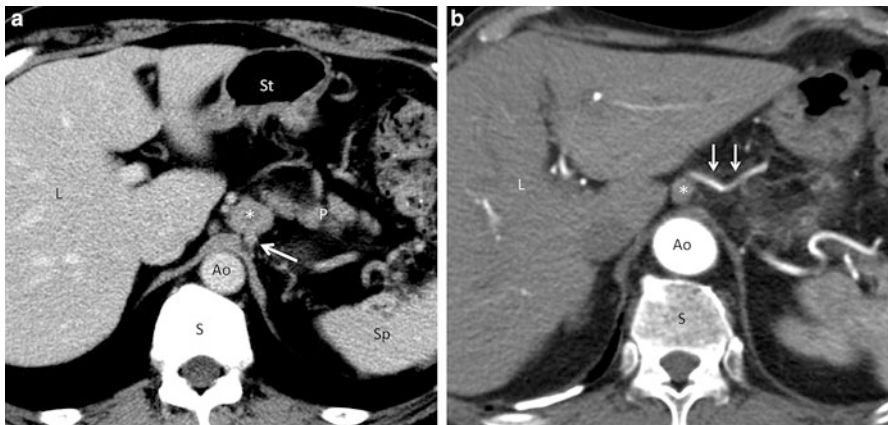


**Fig. 3.18** Metastatic adenopathy of the abdominal nodes. Contrast-enhanced axial CT image (a) of the upper abdomen shows an enlarged lymph node (*asterisk*) adjacent to the celiac trunk (*arrow*). The node contains low attenuation within it. *Ao* aorta, *L* liver, *P* pancreas, *S* spine, *Sp* spleen, *St* stomach. Contrast-enhanced axial CT image (on arterial phase) of the different patients (b) shows an enlarged node (*asterisk*) along the left gastric artery (*arrows*). *Ao* aorta, *L* liver, *S* spine

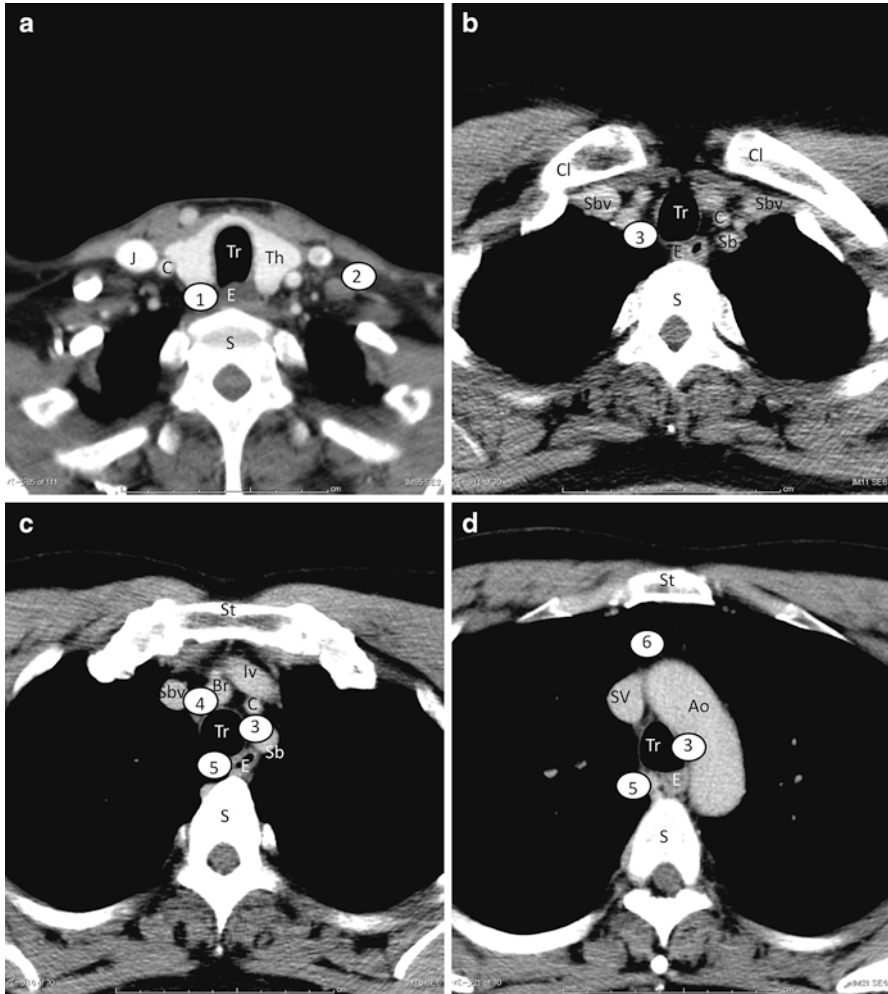


**Fig. 3.19** Representative nodal groups in the lower neck and mediastinum on CT. (a) CT image at the level of the lower neck. (1) cervical paraesophageal node; (2) supraclavicular node. (b) CT image at the level of the thoracic inlet. (3) right recurrent nerve node. (c) CT image at the level of the superior mediastinum. (3) left recurrent nerve node; (4) pretracheal node; (5) upper thoracic paraesophageal node. (d) CT image at the level of the aortic arch. (3) left recurrent nerve node; (5) upper thoracic paraesophageal node; (6) anterior mediastinal node. (e) CT image at the level below the aortic arch. (4) pretracheal node; (5) upper thoracic paraesophageal node; (6) anterior mediastinal node; (7) tracheobronchial node. (f) CT image at the level below the tracheal bifurcation. (8) subcarinal node; (9) middle thoracic paraesophageal node. (g) CT image at the level of the inferior pulmonary vein. (10) lower thoracic paraesophageal node; (11) posterior mediastinal node. (i) CT image at the level just above the diaphragm. (10) lower thoracic paraesophageal node; (11) posterior mediastinal node. AA ascending aorta, Ao aortic arch, Br brachiocephalic vein, C common carotid artery, Cl clavicle, DA descending aorta, E (cervical) esophagus, IP inferior pulmonary vein, Iv innominate vein, IV inferior vena cava, J internal jugular vein, La left atrium, LB left main bronchus, Li liver, LP left pulmonary artery, Lv left ventricle, Pa pulmonary artery main trunk, Ra right atrium, RB right main bronchus, RP right pulmonary artery, Rv right ventricle; Th thyroid gland, Tr trachea; S spine, Sb subclavian artery, Sbv subclavian vein; St sternum, SV superior vena cava

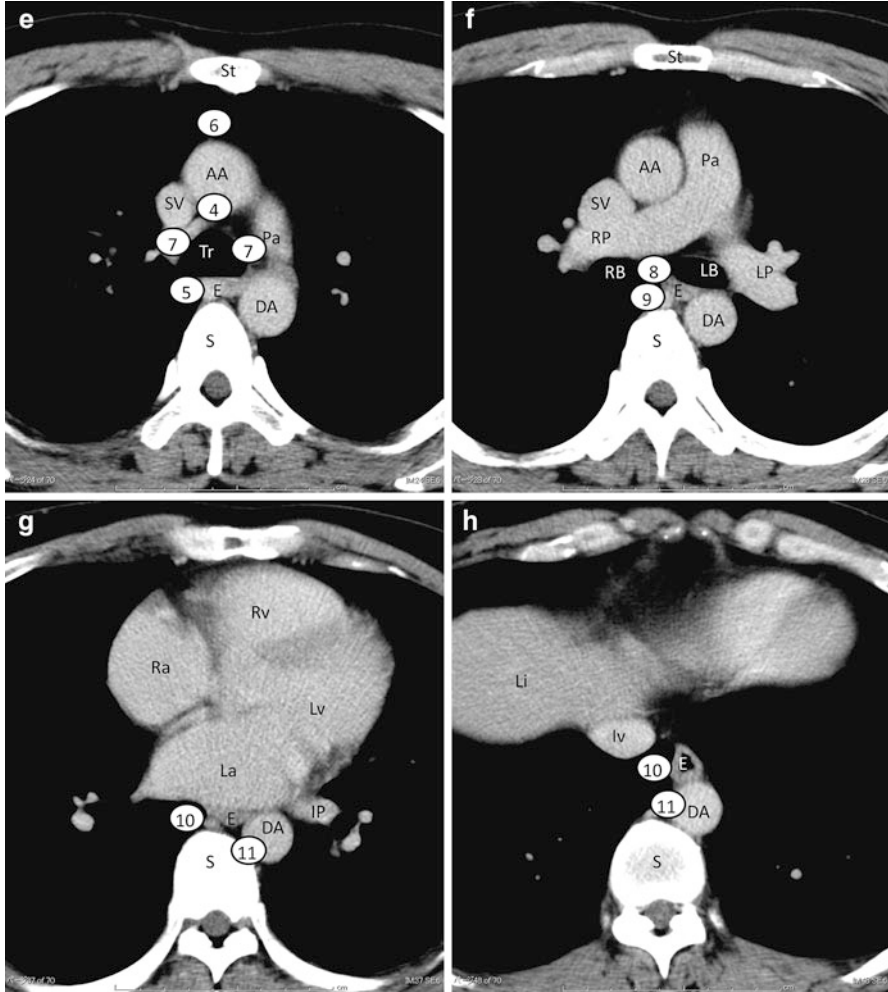


**Fig. 3.19** (continued)

or inflammatory and lymph nodes harbor metastatic foci without significant enlargement. Enlarged paraesophageal nodes near the tumor are sometimes difficult to distinguish from contiguous tumor spread (Fig. 3.20) [15].

Focal defect (intranodal low attenuation) is a reliable feature to determine metastatic adenopathy when identified even in normal-sized nodes (Figs. 3.12, 3.17b, and 3.21).

The sensitivity of CT in detecting mediastinal lymphadenopathy is not high [23]. CT sensitivity and specificity are generally considered as 60–80 % and around 90 %, respectively. Regarding determination of regional lymph node metastases, meta-analysis studies reported that CT showed sensitivity of 50 % and specificity of 83 % and FDG-PET showed sensitivity of 51 % and specificity of 84 %

**Fig. 3.20** Esophageal cancer (lower thoracic esophagus). Contrast-enhanced axial CT image at the level of the lower thoracic esophagus shows an irregularly shaped tumor (*T*). The tumor (*T*) is indistinguishable from enlarged paraesophageal node (*asterisk*) with extranodal spread. *Ao* aorta, *LV* left ventricle, *RA* right atrium, *RV* right ventricle, *S* spine

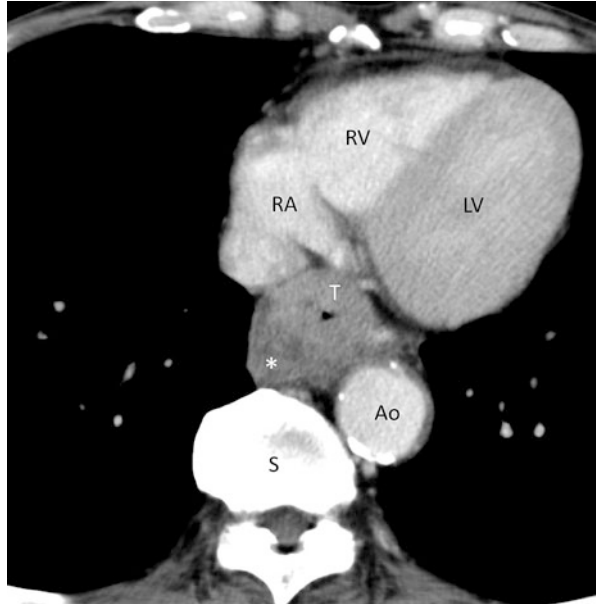


**Fig. 3.21** Esophageal cancer (same patient as Fig. 3.8). Contrast-enhanced axial CT image at the level of the lower thoracic esophagus (*Lt*) shows metastatic adenopathy of the paraesophageal node (*arrow*). Metastatic deposit in the node is manifested by focal defect (intranodal low attenuation). The node is marginal by size criteria. *Ao* aorta, *E* pleural effusion, *LA* left atrium, *LV* left ventricle, *RA* right atrium, *RV* right ventricle, *S* spine



[38, 39]. Lehr reported that the accuracy of CT for diagnosing mediastinal and abdominal lymph nodes was 56 and 45 %, respectively, which are not significantly different from that found with MRI [27].

MRI's role to assess regional nodal metastasis is limited so far although MRI values have improved over the years [24].

### 3.5 M Staging by Imaging

Esophageal cancer is often associated with metastatic deposits at presentation. The distant metastases are most commonly diagnosed in the abdominal lymph nodes (Fig. 3.18) [39]. Hematogenous metastases, often found in patients with esophageal cancer, commonly involve the liver (Fig. 3.22a), lung (Fig. 3.22b),

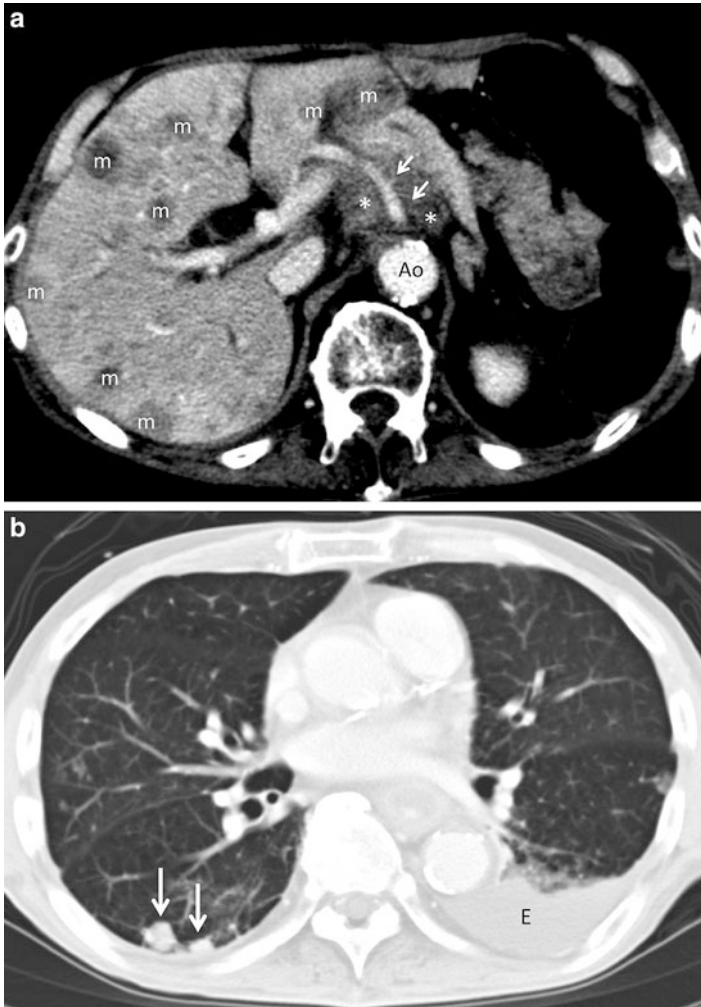


**Fig. 3.22** Distant metastases to the liver and lungs. (a) Contrast-enhanced axial CT image of the liver on delayed/portal phase. There are numerous metastatic deposits (*m*) in the liver. Enlarged abdominal nodes (*asterisk*) encase the celiac artery (*arrows*). (b) Axial CT image in lung window of the same patient. Metastatic lung tumors are manifested by several round-shaped nodules (*arrows*) in the right lower lobe. Pleural effusion (*E*) is noted on the *left side*

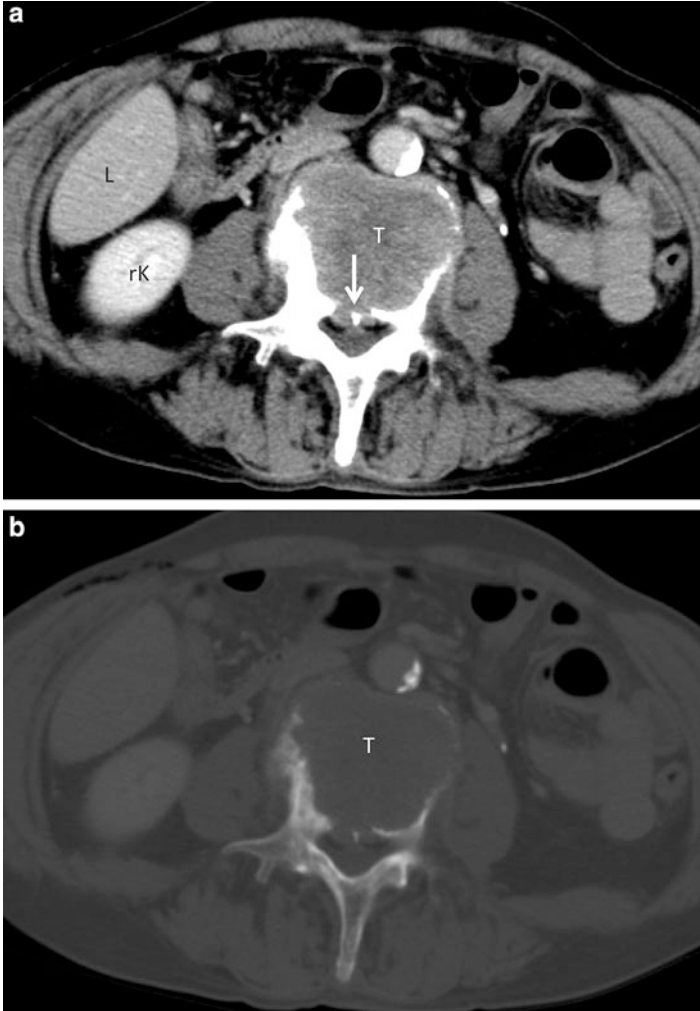


**Fig. 3.23** Distant metastasis to the 4th lumbar spine. Axial CT image in soft tissue window (**a**) and bone window (**b**) shows a destructive lesion (*T*) of the 4th lumbar spine. Posteriorly, the lesion protrudes into the anterior aspect of the spinal canal (*arrows*) with impingement upon the anterior aspect of dural sac. *L* liver, *rK* right kidney

bone (Fig. 3.23), adrenal gland, kidney, and brain in descending order of frequency of occurrence [5, 40, 41].

Early detection of distant metastatic foci is important for the accurate staging and appropriate treatment plan. CT is the most commonly used on this purpose. Neither MR nor CT is sensitive in detecting metastases to distant nodes, but the specificity is high [28]. CT is currently the best diagnostic method to detect metastases and may also reveal enlarged lymph nodes around the celiac axis [12].

CT depicts metastatic deposits in the liver as low-attenuation areas on non-contrast and post-contrast images, best visualized on the portal/delayed phases (Fig. 3.22a). CT also depicts metastatic lung tumors as, usually rounded, smoothly bordered and non-calcific, nodules and/or masses (Fig. 3.22b). CT of the lung field window setting is suitable for the evaluation.

PET is a powerful tool and more sensitive than CT for the detection of distant metastases [42]. PET can reveal metastatic diseases in 15 % of patients who were considered to be without distant disease only on the basis of findings on conventional diagnostic modalities [43, 44]. The major problems with FDG-PET staging of esophageal cancer are failure to detect metastatic deposits less than 1 cm in diameter and lack of anatomic definition [45].

---

### 3.6 Follow-Up

Imaging is commonly used to follow-up esophageal cancers during therapy and document response. Whereas EUS and barium esophagography may show response of the primary lesion, CT is useful to reveal response of not only the primary lesion but also the regional and distant metastases [35]. CT is considered complementary to EUS and barium esophagography on this purpose.

The ability to detect local recurrence is variable because inflammation or fibrosis may cause anatomical distortion and esophageal wall thickening, mimicking local recurrence on imaging [35]. Comparison with baseline study is mandatory to early detection of recurrent disease. The overall accuracy of CT in detecting recurrence is reported to be 87 % [46].

---

### References

1. American Joint Committee on Cancer (2010) Edge SB et al (ed) AJCC Cancer Staging Manual seventh edition Springer-Verlag, New York
2. Mancuso AA (2011) Cervical esophagus. In: Mancuso AA (ed) Head and neck radiology. Lippincott Williams & Wilkins, a Wolters Kluwer, Philadelphia
3. Hasegawa N, Niwa Y, Arisawa T et al (1996) Preoperative staging of superficial esophageal carcinoma: comparison of an ultrasound probe and standard endoscopic ultrasonography. *Gastrointest Endosc* 39:388–392
4. Postlethwait RW (1983) Carcinoma of the thoracic esophagus. *Surg Clin North Am* 63:933–940
5. Kim TJ, Kim HY, Lee KW et al (2009) Multimodality assessment of esophageal cancer: preoperative staging and monitoring of response to therapy. *Radiographics* 29:403–421
6. Levine MS, Rubesin SE (2005) Diseases of the esophagus: diagnosis with esophagography. *Radiology* 237:414–427
7. The Japan Esophageal Society (2008) Japanese classification of esophageal cancer, 10th edn. Kanehara Co. Ltd, Tokyo
8. Levine MS, Chu P, Furth EE et al (1997) Carcinoma of the esophagus and esophagogastric junction: sensitivity of radiographic diagnosis. *AJR Am J Roentgenol* 168:1423–1426
9. Levine MS, Halvorsen RA (1994) Esophageal carcinoma. In: Core RM, Levine MS, Laufer I (eds) *Textbook of gastrointestinal radiology*. WB Saunders Co, Philadelphia

10. Wakelin SJ, Deans C, Crofts TJ et al (2002) A comparison of computerized tomography, laparoscopic ultrasound and endoscopic ultrasound in the preoperative staging of oesophago-gastric carcinoma. *Eur J Radiol* 41:161–167
11. Preston ST, Clark GW, Martin IG et al (2003) Effect of endoscopic ultrasonography on the management of 100 consecutive patients with oesophageal and junctional carcinoma. *Br J Surg* 90:1220–1224
12. Holscher AH, Dittler HJ, Siewert JR (1994) Staging of squamous esophageal cancer: accuracy and value. *World J Surg* 18:312–320
13. van den Hoed RD, Feldberg MAM, van Leeuwen MS et al (1997) CT prediction of irresectability in esophageal carcinoma: value of additional patient positions and relation to patient outcome. *Abdom Imaging* 22:132–137
14. Thompson WM, Halvorsen RA, Foster WL Jr et al (1983) Computed tomography for staging esophageal and gastroesophageal cancer: reevaluation. *AJR Am J Roentgenol* 141:951–958
15. Halvorsen RA Jr, Thompson WM (1987) Computed tomographic staging of gastrointestinal malignancies. I. Esophagus and stomach. *Invest Radiol* 22:2–16
16. Umeoka S, Koyama T, Togashi K et al (2006) Esophageal cancer: evaluation with triple-phase dynamic CT – initial experience. *Radiology* 239:777–783
17. Umeoka S, Okada T, Daido S et al (2013) “Early esophageal rim enhancement”: a new sign of esophageal cancer on dynamic CT. *Eur J Radiol* 82:459–463
18. Yoon YC, Lee KS, Shim YM et al (2003) Metastasis to regional lymph nodes in patients with esophageal squamous cell carcinoma: CT versus FDG PET for presurgical detection prospective study. *Radiology* 227:764–770
19. Desai RK, Tagliabue JR, Wegryn SA et al (1991) CT evaluation of wall thickening in the alimentary tract. *Radiographics* 11:771–783
20. Xia F, Mao J, Ding J, Yang H (2009) Observation of normal appearance and wall thickness of esophagus on CT images. *Eur J Radiol* 72:406–411
21. Liao ZX, Liu H, Komaki R (2003) Target delineation for esophageal cancer. *J Women’s Imaging* 5:177–186
22. Moss AA, Schnyder P, Thoeni RF et al (1981) Esophageal carcinoma: pretherapy staging by computed tomography. *Am J Roentgenol* 136:1051–1056
23. Noh HM, Fishman EK, Forastiere AA et al (1995) CT of the esophagus: spectrum of disease with emphasis on esophageal carcinoma. *Radiographics* 15:1113–1134
24. Van Rossum PSN, van Hillegersberg R, Lever FM et al (2013) Imaging strategies in the management of oesophageal cancer: what’s the role of MRI? *Eur Radiol* 23:1753–1765
25. Picus D, Balfé DM, Koehler RE et al (1983) Computed tomography in the staging of esophageal carcinoma. *Radiology* 46:433–438
26. Daffner RH, Halber MD, Postlethwait RW et al (1979) CT of the esophagus. II. Carcinoma. *AJR Am J Roentgenol* 133:1051–1055
27. Lehr L, Rupp N, Siewert JR (1988) Assessment of resectability of esophageal cancer by computed tomography and magnetic resonance imaging. *Surgery* 103:344–350
28. Takashima S, Takeuchi N, Shiozaki H et al (1991) Carcinoma of the esophagus: CT vs MR imaging in determining resectability. *AJR Am J Roentgenol* 156:297–302
29. Quint LE, Bogot NR (2008) Staging esophageal cancer. *Cancer Imag* 8:S33–S42, Sepc No A
30. Lefor AT, Merino MM, Steinberg SM et al (1989) Computerized tomographic prediction of extraluminal spread and prognostic implications of lesion width in esophageal cancer (abstr). *Radiology* 171:290
31. Ruf G, Brobmann GF, Grosser G et al (1985) Wert der Computer-tomographie für die Beurteilung der lokalen Operabilität und die chirurgische Verfahrenswahl beim Oesophaguscarcinom. *Langenbecks Arch Chir* 365:157–168
32. Ogawa Y, Nischiyama K, Ikese J et al (1987) Preoperative assessment of tumor invasions of the intrathoracic esophageal carcinoma. In: Siewert JR, Holscher AH (eds) *Diseases of the esophagus*, 1st edn. Springer, New York, pp 203–206

33. Sakurada A, Takahara T, Kwee IC et al (2009) Diagnostic performance of diffusion-weighted magnetic resonance imaging in esophageal cancer. *Eur Radiol* 19:1461–1469
34. Tio TL, Cohen P, Coene PP et al (1987) Endosonography and computed tomography of esophageal carcinoma; preoperative classification compared to the new (1987) TNM system. *Gastroenterology* 96:1478–1486
35. Iyer RB, Silverman PM, Tamm EP et al (2003) Imaging in oncology from the University of Texas M.D. Anderson Cancer Center. Diagnosis, staging, and follow-up of esophageal cancer. *AJR Am J Roentgenol* 181:785–793
36. Block MI, Patterson GA, Sundaresan RS et al (1997) Improvement in staging of esophageal cancer with the addition of positron emission tomography. *Ann Thorac Surg* 64:770–777
37. Kato H, Kuwano H, Nakajima M et al (2002) Comparison between positron emission tomography and computed tomography in the use of the assessment of esophageal carcinoma. *Cancer* 94:921–928
38. Van Vliet EP, Heijnenbroek-Kal MH, Hunink MG et al (2008) Staging investigation for oesophageal cancer: a meta-analysis. *Br J Cancer* 98:547–557
39. Van Westreenen HL, Westerterp M, Bossuyt PM et al (2004) Systematic review of the staging performance of 18F-fluorodeoxyglucose positron emission tomography in esophageal cancer. *J Clin Oncol* 22:3805–3812
40. Quint LE, Hepburn LM, Francis IR et al (1995) Incidence and distribution of distant metastases from newly diagnosed esophageal carcinoma. *Cancer* 76:1120–1125
41. Mandard AM, Chasle J, Marnay J et al (1981) Autopsy findings in 111 cases of esophageal cancer. *Cancer* 48:329–335
42. Flanagan FL, Dehdashti F, Siegel BA et al (1997) Staging of esophageal cancer with 18F-fluorodeoxyglucose positron emission tomography. *AJR Am J Roentgenol* 168:417–424
43. Flamen P, Lerut A, Van Cutsem E et al (2000) Utility of positron emission tomography for the staging of patients with potentially operable esophageal carcinoma. *J Clin Oncol* 18:3202–3210
44. Downey RJ, Akhurst T, Ilson D et al (2003) Whole body 18FDG-PET and the response of esophageal cancer to induction therapy: results of the prospective trial. *J Clin Oncol* 21:428
45. Rice TW (2000) Clinical staging of esophageal carcinoma. CT, EUS, and PET. *Chest Surg Clin N Am* 10:471–485
46. Carlisle JG, Quint LE, Francis IR et al (1993) Recurrent esophageal carcinoma: CT evaluation after esophagectomy. *Radiology* 189:271–275